Polarisation Orientation Effects and Hydrostatic Parameters in Novel 2–2 Composites Based on PMN–*x*PT Single Crystals

C. R. BOWEN[1,*] AND V. YU. TOPOLOV[2]

[1] Department of Mechanical Engineering, University of Bath, BA2 7AY Bath, United Kingdom

[2] Department of Physics, Southern Federal University, 344090 Rostov-on-Don, Russia

Polarisation orientation effects in piezo-active composites based on relaxor-ferroelectric single crystals of $(1 - x)Pb(Mg_{1/3}Nb_{2/3})O_3–xPbTiO_3$ *open up new possibilities to vary the effective electromechanical properties and related parameters. In the present paper the hydrostatic performance of 2–2 parallel-connected single crystal / auxetic polymer composites is studied for* $x = 0.28–0.33$ *and two poling directions of the single-crystal component, [001] (4mm symmetry) and [011] (mm2 symmetry) in the perovskite unit cell. The effect of the orientation of the main crystallographic axes in the single-crystal component on the hydrostatic piezoelectric coefficients* d_h^*, e_h^* *and squared figure of merit* $d_h^* g_h^*$ *is analysed for three rotation modes in single crystals and at various anisotropy of their piezoelectric and elastic properties. The role of the auxetic polymer component is emphasised in the context of the large hydrostatic parameters and anisotropy of squared figures of merit* $d_{3j}^* g_{3j}^*$ $(j = 1, 2 \text{ and } 3)$. *The largest maximum values of* d_h^* *and* e_h^* *(1990 pC / N and 42.5 C / m*^{2}*, respectively) are achieved in the composite based on [011]-poled* $0.71Pb(Mg_{1/3}Nb_{2/3})O_3–0.29PbTiO_3$.

Keywords: Composite; Ferroelectric; Crystallographic orientation; Hydrostatic piezoelectric response; Figures of merit

PACS: 77.65.-j: Piezoelectricity and electromechanical effects; 77.84.Lf: Composite materials; 77.84.-s: Dielectric; piezoelectric; ferroelectric; and antiferroelectric materials

* Corresponding author. E-mail: C.R.Bowen@bath.ac.uk

1. Introduction

Domain-engineered single crystals (SCs) of relaxor-ferroelectric $(1 - x)Pb(Mg_{1/3}Nb_{2/3})O_3 - xPbTiO_3$ (PMN–*x*PT) with the perovskite-type structure are of interest as components of advanced piezo-active composites [1–3]. The PMN–*x*PT SCs with compositions near the morphotropic phase boundary ($x \approx 0.3$) exhibit remarkable electromechanical (i.e., piezoelectric, elastic and dielectric) properties (Table 1) that are measured [4–7] on samples poled along specific crystallographic directions which may be varied in a wide range due to a polarisation orientation effect [3]. A change in a poling direction leads to changes in a piezoelectric activity and anisotropy of the properties of the SC component that influences the properties of the related composite. Modern PMN–*x*PT SC / polymer composites with 1–3 and 2–2 connectivity patterns [1, 3] are regarded as novel piezo-active materials with many parameters suitable for piezotechnical, hydroacoustic and energy harvesting applications. Among these materials the 2–2 (laminar) composites are important objects for a study of the orientation effects [3, 8] and interconnections between the properties of the SC component and composite as a whole. To the best of our knowledge, data on the hydrostatic piezoelectric performance have yet to be systematised for the 2–2 PMN–*x*PT-based composites at various *x* and orientations of the main crystallographic axes of the SC component. An additional stimulus to improve the hydrostatic parameters is to employ a auxetic polymer component with a negative Poisson's ratio [8, 9]. The aim of the present paper is to study the hydrostatic piezoelectric response and related parameters of the 2–2 PMN–*x*PT SC / auxetic polyethylene composites with $x = 0.28–0.33$ at taking into account the orientation effect in the [001]- and [011]-poled SCs.

2. Model of the 2–2 Composite and Their Effective Parameters

A 2–2 parallel-connected composite with a regular distribution of layers on the OX_1 direction (Fig. 1) comprises the SC and polymer layers distributed continuously over the OX_2 and OX_3 directions. An orientation of the spontaneous polarisation vector $\boldsymbol{P}_s^{(1)}$ in each single-domain SC layer is shown in inset 1 (SC poled along [001] of the perovskite unit cell) and inset 2 (SC poled along [011] of the perovskite unit cell) of Fig. 1. Following results in [3], we consider a rotation

of the main crystallographic axes x, y and z of the polydomain SC layer around one of the co-ordinate axes – $OX_1 \parallel$ x (inset 3 in Fig. 1), $OX_2 \parallel$ y (inset 4 in Fig. 1) or $OX_3 \parallel$ z (inset 5 in Fig. 1). Such rotation modes enable us to maintain polydomain states (insets 1 and 2 in Fig. 1) and to study the orientation effects in the presence of the [001]- and [011]-poled SCs. We assume that at these rotation modes, the spontaneous polarisation vectors of domains $\boldsymbol{P}_{s,1}$, $\boldsymbol{P}_{s,2}$ etc. in each SC layer are situated either over or in the (X_1OX_2) plane (Fig. 1). Hereby the rotation angles are varied [3] as follows:

(i) $-45° \le \alpha \le 45°$ or $-45° \le \beta \le 45°$ (composite based on the [001]-poled SC, rotation modes in insets 3 and 4 in Fig. 1) and

(ii) $-\arcsin(1/\sqrt{3}) \le \alpha \le \arcsin(1/\sqrt{3})$, $-45° \le \beta \le 45°$ or $0° \le \gamma \le 360°$ (composite based on the [011]-poled SC, rotation modes in insets 3–5 in Fig. 1).

Because of the 4*mm* symmetry of the [001]-poled polydomain SC [4–6] and $d_{31}^{(1)} = d_{32}^{(1)}$ for this symmetry class, we do not consider the rotation of the main crystallographic axes x, y and z around $OX_3 \parallel$ z in the case (i).

The effective electromechanical properties of the 2–2 composite are evaluated using the complete sets of electromechanical constants of SCs (Table 1) and polymer*. Averaging the electromechanical properties along the OX_1 axis is performed by taking into consideration boundary conditions [2, 3] for electric and mechanical fields in the adjacent layers of the composite sample (Fig. 1). These boundary conditions at x_1 = const involve the continuity of three normal components of the mechanical stress (σ_{11}, σ_{12} and σ_{13}), three tangential components of the mechanical strain (ξ_{22}, ξ_{23} and ξ_{33}), one normal component of the electric displacement (D_1), and two tangential components of the electric field (E_2 and E_3). The effective properties of the 2–2 composite are represented by the matrix

$$\| C^* \| = [\| C^{(1)} \| \cdot \| M \| m + \| C^{(2)} \| (1 - m)] [\| M \| m + \| I \| (1 - m)]^{-1}, \qquad (1)$$

---

* Auxetic polyethylene is a piezo-passive polymer with elastic compliances $s_{11}^{(n)} = 5260$ and $s_{12}^{(n)} = 4360$ (in 10^{-12} Pa^{-1}) [10] and dielectric permittivity $\varepsilon_{pp}^{(n)} / \varepsilon_0 = 2.3$ [11] at room temperature.

where $\| C^{(n)} \| = \begin{pmatrix} \| s^{(n),E} \| & \| d^{(n)} \|^T \\ \| d^{(n)} \| & \| \varepsilon^{(n),\sigma} \| \end{pmatrix}$ (9×9 matrix) describes the properties of SC (n = 1) and polymer (n = 2), and superscript 'T' denotes the transposed matrix. In Eq. (1) $\| M \|$ is the 9×9 matrix concerned with the boundary conditions at x_1 = const, $\| I \|$ is the 9×9 identity matrix, and m is the volume fraction of the SC component. Thus, the studied 2–2 composite (Fig. 1) is characterised by the full set of electromechanical constants s_{ab}^{*E}, d_{ij}^{*} and $\varepsilon_{fh}^{*\sigma}$ from $\| C^* \|$ in Eq. (1). These constants are determined in the longwave approximation [2], when the wavelength of the external acoustic field is much greater than the width of each layer of the sample.

3. Orientation Effects and Improved Parameters in PMN–*x*PT-Based Composites

Hydrostatic parameters $\Pi_h^*(m, \alpha)$, $\Pi_h^*(m, \beta)$ and $\Pi_h^*(m, \gamma)$ are studied for the composite in Fig. 1 with electrodes that are parallel to the (X_1OX_2) plane, and therefore, the piezoelectric coefficients with subscripts 31, 32 and 33 are to be considered. Among Π_h^*s to be discussed, of interest for applications are the hydrostatic piezoelectric coefficients

$$d_h^* = d_{31}^* + d_{32}^* + d_{33}^*, \; g_h^* = g_{31}^* + g_{32}^* + g_{33}^* \text{ and } e_h^* = e_{31}^* + e_{32}^* + e_{33}^* \tag{2}$$

and squared hydrostatic figure of merit

$$(Q_h^*)^2 = d_h^* \, g_h^*, \tag{3}$$

where g_{ij}^* and e_{ij}^* from Eqs. (2) are determined using formulae [12] $\| g^* \| = \| d^* \| \cdot \| \varepsilon^{*\sigma} \|^{-1}$ and $\| e^* \| = \| d^* \| \cdot \| s^{*E} \|^{-1}$, respectively. The hydrostatic piezoelectric coefficients d_h^*, g_h^* and e_h^* from Eqs. (2) provide a measure of the activity and sensitivity of the composite [2] under hydrostatic loading. $(Q_h^*)^2$ from Eq. (3) is used to characterise the sensor signal-to-noise ratio of the composite and its piezoelectric sensitivity [2]. $(Q_h^*)^2$ is analogous to squared figures of merit $(Q_{3j}^*)^2$ (j = 1, 2 and 3) [8] which are of value for modern energy harvesting applications.

As follows from data on absolute maxima of Π_h^* (Table 2),

(i) absolute max d_h^* in the composite based on the [001]-poled SC correlates with $d_h^{(1)}$ of the SC,

(ii) the largest value of absolute max d_h^* is achieved in the composite based on the [011]-poled SC with the largest value of $|d_h^{(1)}|$ (see Table 1, $x = 0.29$),

(iii) changes in the rotation angle β lead to the larger values of absolute max e_h^* in the composite based on the [001]-poled SC (Table 2), however no distinct correlation between max e_h^* and $|e_h^{(1)}|$ from Table 1 is seen in this case, and

(iv) the largest value of absolute max e_h^* is achieved due to the large piezoelectric coefficients $d_{ij}^{(1)}$, their anisotropy and the elastic anisotropy of the [011]-poled SC with $x = 0.29$ (Table 1).

Absolute maxima of $(Q_h^*)^2$ and $(Q_{3j}^*)^2$ in the studied composites are achieved at small volume fractions of SC ($0 < m < 0.02$), and therefore, it would be difficult to manufacture the requested composite samples within this m range. The volume-fraction behaviour of local maxima of $(Q_h^*)^2$ and $(Q_{33}^*)^2$ is similar (Fig. 2), and their decrease is caused by a rapid increase of $\varepsilon_{33}^{*\sigma}$ on increasing m. The inequality $(Q_h^*)_m{}^2 > (Q_{33}^*)_m{}^2$ holds at $m < 0.1$ (Fig. 2), i.e., there is a strong influence of the auxetic polymer component on the effective properties.

It is noteworthy that the condition

$$(Q_{33}^*)^2 / (Q_{3j}^*)^2 \geq 10 \ (j = 1 \text{ and } 2) \qquad (4)$$

holds within a wide range of volume fraction m and rotation angles, in the presence of the SC component poled either along [001] (Fig. 3, a) or [011] (Fig. 3, b) and at different rotation modes. A considerable part of the hatched area in Fig. 3, a is related to (m, α) that provides a large $(Q_h^*)_m{}^2$ (see curve 3 in Fig. 2). This performance is due to the orientation effect and elastic anisotropy in the studied composite and the relatively high piezoelectric activity of its SC component. It should be added that $(Q_{33}^{(1)})^2 / (Q_{31}^{(1)})^2 = (Q_{33}^{(1)})^2 / (Q_{32}^{(1)})^2 = (d_{33}^{(1)} / d_{31}^{(1)})^2 \approx 4.5$ is related to the [001]-poled PMN–0.33PT SC (see data in Table 1).

We note that data on d_h^*, g_h^* and $(Q_h^*)_m{}^2$ (Table 2 and Fig. 2) highlight the advantages of these particular composites over conventional 2–2 PZT-type ceramic / polymer composites with

$\max d_h^*$ ≈ (50–80) pC / N and $\max g_h^*$ ≈ (100–300) mV·m / N [13]. Experimental values of $\max[(Q_h^*)^2] \approx 5 \cdot 10^{-11}$ Pa^{-1} are peculiar to a 2–2 PZT-type ceramic / polymer composite [14] with a specific orientation of the layers with respect to the poling direction. Values of absolute $\max e_h^*$ (Table 2) are about 2–4 times larger than typical values of e_h ≈ (10–15) C / m^2 in PZT-type ceramics [2].

4. Conclusions

Features of the hydrostatic piezoelectric response of the 2–2 PMN–*x*PT SC / auxetic polyethylene composite (x = 0.28–0.33) have been studied taking into account the orientation effect in the [001]- and [011]-poled SCs and the role of the auxetic polymer. The orientation of the main crystallographic axes in the SC layer and the anisotropy of its piezoelectric and elastic properties are to be taken into account for the manufacture of the novel piezo-active composites with large values of d_h^*, e_h^* and $(Q_h^*)^2$. Both the [001]- and [011]-poled SCs (Table 1) have individual advantages at different rotation modes. The auxetic polymer component with $\operatorname{sgn} s_{11}^{(2)} = \operatorname{sgn} s_{12}^{(2)} > 0$ strongly influences d_{3j}^* and hydrostatic parameters (2) and (3). Examples of validity of condition (4) testify to the important role of the piezoelectric anisotropy and orientation effects at different rotation modes. In general, the studied orientation effects promote the large hydrostatic parameters and anisotropy of squared figures of merit (4), and these characteristics are of value for hydroacoustic, energy harvesting and related applications.

Acknowledgements

Prof. Bowen acknowledges funding from the European Research Council under the European Union's Seventh Framework Programme (FP/2007-2013) / ERC Grant Agreement no. 320963 on Novel Energy Materials, Engineering Science and Integrated Systems (NEMESIS). The research subject is concerned with the Programme Supporting the Research at the Southern Federal University (Russia). The authors would like to thank Prof. Dr. R. Stevens (University of Bath, UK), Prof. Dr. A. E. Panich, Prof. Dr. I. A. Parinov and Prof. Dr. A. A. Nesterov (Southern Federal University, Russia) for their continuing interest in the research problems.

References

1. F. Wang, C. He, Y. Tang, X. Zhao, and H. Luo, Single-crystal 0.7Pb($Mg_{1/3}Nb_{2/3}$)O_3–0.3$PbTiO_3$/epoxy 1–3 piezoelectric composites prepared by the lamination technique. *Mater. Chem. Phys*. **105**, 273–277 (2007).

2. V. Yu. Topolov and C. R. Bowen, *Electromechanical Properties in Composites Based on Ferroelectrics*. London: Springer (2009).

3. V. Yu. Topolov, C. R. Bowen, and A. V. Krivoruchko, Role of domain orientations in forming the hydrostatic performance of novel 2–2 single crystal/polymer composites. *Ferroelectrics* **444**, 84–99 (2013).

4. G. Liu, W. Jiang, J. Zhu, and W. Cao, Electromechanical properties and anisotropy of single- and multi-domain 0.72Pb($Mg_{1/3}Nb_{2/3}$)O_3-0.28$PbTiO_3$ single crystals. *Appl. Phys. Lett*. **99**, 162901 – 3 p. (2011).

5. R. Zhang, W. Jiang, B. Jiang, and W. Cao, Elastic, dielectric and piezoelectric coefficients of domain engineered 0.70Pb($Mg_{1/3}Nb_{2/3}$)O_3 – 0.30$PbTiO_3$ single crystal. In: *Fundamental Physics of Ferroelectrics*, Ed. R. E. Cohen. Melville: American Institute of Physics; 188–197 (2002).

6. R. Zhang, B. Jiang, and W. Cao, Elastic, piezoelectric, and dielectric properties of multidomain 0.67Pb($Mg_{1/3}Nb_{2/3}$)O_3–0.33$PbTiO_3$ single crystals. *J. Appl. Phys*. **90**, 3471–3475 (2001).

7. F. Wang, L. Luo, D. Zhou, X. Zhao, and H. Luo, Complete set of elastic, dielectric, and piezoelectric constants of orthorhombic 0.71Pb($Mg_{1/3}Nb_{2/3}$)O_3–0.29$PbTiO_3$ single crystal. *Appl. Phys. Lett*. **90**, 212903 – 3 p. (2007).

8. C. R. Bowen, V. Yu. Topolov, D. N. Betts, and H. A. Kim, 2–2 composites based on [011]-poled relaxor-ferroelectric single crystals: from the piezoelectric activity to the hydrostatic response. *Proc. SPIE* **8763**, 876320 – 10 p. (2013).

9. V. Yu. Topolov, A. V. Krivoruchko, and C. R. Bowen, Anisotropy of electromechanical properties and hydrostatic response of advanced 2–2-type composites. *Phys. Stat. Sol. A* **209**, 1334–1342 (2012).

10. K. E. Evans, and K. L. Alderson, The static and dynamic moduli of auxetic microporous polyethylene. *J. Mater. Sci. Lett*. **11**, 1721–1724 (1992).

11. I. N. Groznov, Dielectric permittivity. In: *Physics Encyclopaedia*. Moscow: Sovetskaya Entsiklopediya; 178–179 (in Russian) (1983).

12. T. Ikeda, *Fundamentals of Piezoelectricity*. Oxford, New York, Toronto: Oxford University Press (1990).

13. A. A. Grekov, S. O. Kramarov, and A. A. Kuprienko, Anomalous behavior of the two-phase lamellar piezoelectric texture. *Ferroelectrics* **76**, 43–48 (1987).

14. A. Safari and E. K. Akdogan, Rapid prototyping of novel piezoelectric composites. *Ferroelectrics* **331**, 153–179 (2006).

Table 1. Elastic compliances $s_{ab}^{(n),E}$ (in 10^{-12} Pa^{-1}), piezoelectric coefficients $d_{ij}^{(n)}$, $d_h^{(n)}$ (in pC / N) and $e_h^{(n)}$ (in C / m^2), hydrostatic squared figure of merit $(Q_h^{(n)})^2$ (in 10^{-12} Pa^{-1}), and dielectric permittivity $\varepsilon_{pp}^{(n),\sigma}$ of domain-engineered PMN–*x*PT SCs at room temperature. Data are related to the main crystallographic axes

	[001]-poled SC, x = 0.28, 4*mm* symmetry [4]	[001]-poled SC, x = 0.30, 4*mm* symmetry [5]	[001]-poled SC, x = 0.33, 4*mm* symmetry [6]	[011]-poled SC, x = 0.28, *mm*2 symmetry [4]	[011]-poled SC, x = 0.29, *mm*2 symmetry [7]
$s_{11}^{(n),E}$	44.57	52.0	69.0	13.40	18.0
$s_{12}^{(n),E}$	–28.91	–18.9	–11.1	–21.18	–31.1
$s_{13}^{(n),E}$	–13.91	–31.1	–55.7	12.67	8.4
$s_{22}^{(n),E}$	44.57	52.0	69.0	54.36	11.2
$s_{23}^{(n),E}$	–13.91	–31.1	–55.7	–33.59	–61.9
$s_{33}^{(n),E}$	34.38	67.7	119.6	28.02	49.6
$s_{44}^{(n),E}$	15.22	14.0	14.5	15.22	14.9
$s_{55}^{(n),E}$	15.22	14.0	14.5	147.06	69.4
$s_{66}^{(n),E}$	16.34	15.2	15.2	22.47	13.0
$d_{15}^{(n)}$	122	190	146	2162	1188
$d_{24}^{(n)}$	122	190	146	160	167
$d_{31}^{(n)}$	–569	–921	–1330	447	610
$d_{32}^{(n)}$	–569	–921	–1330	–1150	–1883
$d_{33}^{(n)}$	1182	1981	2820	860	1030
$\varepsilon_{11}^{(n),\sigma} / \varepsilon_0$	1672	3600	1600	4235	3564
$\varepsilon_{22}^{(n),\sigma} / \varepsilon_0$	1672	3600	1600	1081	1127
$\varepsilon_{33}^{(n),\sigma} / \varepsilon_0$	5479	7800	8200	3873	4033
$d_h^{(n)}$ [a]	44	139	160	157	–243
$e_h^{(n)}$	–23.5	22.2	15.5	14.3	22.5
$(Q_h^{(n)})^2$	0.0399	0.280	0.353	0.719	1.654

[a] $d_h^{(n)}$, $e_h^{(n)}$ and $(Q_h^{(n)})^2$ were calculated using values of $d_{3j}^{(n)}$, $s_{kl}^{(n),E}$ and $\varepsilon_{33}^{(n),\sigma}$

Table 2. Absolue maxima of hydrostatic piezoelectric coefficients d_h^* and e_h^* in the 2–2 PMN–*x*PT SC / auxetic PE composite at rotation modes shown in insets 3–5 in Fig. 1

SC poling direction	x	Absolute max d_h^*		Absolute max e_h^*	
		Value (in pC / N)	Rotation angle and volume fraction of SC	Value (in C / m^2)	Rotation angle and volume fraction of SC
[001]	0.28	939	α = 0°, m = 0.029	29.2	β = ±25°, m = 0.872
	0.30	1210	α = 0°, m = 0.101	39.3	β = ±33°, m = 0.872
	0.33	1410	α = 0°, m = 0.177	29.7	β = ±33°, m = 0.865
[011]	0.28	1650	γ = 0°, m = 0.074	30.8	γ = 90°, m = 0.941
	0.29	1990	γ = 0°, m = 0.072	42.5	γ = 65° or 115°, m = 0.890

Figure captions to the paper "Polarisation Orientation Effects and Hydrostatic Parameters in Novel 2–2 Composites Based on PMN–*x*PT Single Crystals"

by C. R. Bowen and V. Yu. Topolov

Fig. 1. Schematic of the 2–2 SC / polymer composite with parallel-connected layers. ($X_1X_2X_3$) is a rectangular co-ordinate system. Inset 1 comprises domain orientations in the [001]-poled SC with the effective spontaneous polarisation vector $\boldsymbol{P}_s^{(1)}$, and inset 2 comprises domain orientations in the [011]-poled SC with the effective spontaneous polarisation vector $\boldsymbol{P}_s^{(1)}$. $\boldsymbol{P}_{s,1}$, $\boldsymbol{P}_{s,2}$, $\boldsymbol{P}_{s,3}$, and $\boldsymbol{P}_{s,4}$ are spontaneous polarisation vectors of several domain types, x, y and z are the main crystallographic axes of the polydomain SC. In inset 1 x, y and z are parallel to the co-ordinate axes OX_1, OX_2 and OX_3, respectively. α, β and γ are angles of rotation of the main crystallographic axes and spontaneous polarisation vectors $\boldsymbol{P}_{s,n}$ in the SC layer around one of the co-ordinate axes OX_j (insets 3–5).

Fig. 2. Local maxima of squared figures of merit $(Q_h^*)_m^2$ and $(Q_{33}^*)_m^2$ (in 10^{-12} Pa^{-1}) of the 2–2 PMN–*x*PT SC / auxetic PE composite with SC layers poled along [001].

Fig. 3. Examples of validity of condition (4) (hatched areas in graphs) at different rotation modes in the 2–2 PMN–*x*PT SC / auxetic PE composite: a, $x = 0.33$ and SC layers poled along [001], and b, $x = 0.29$ and SC layers poled along [011].

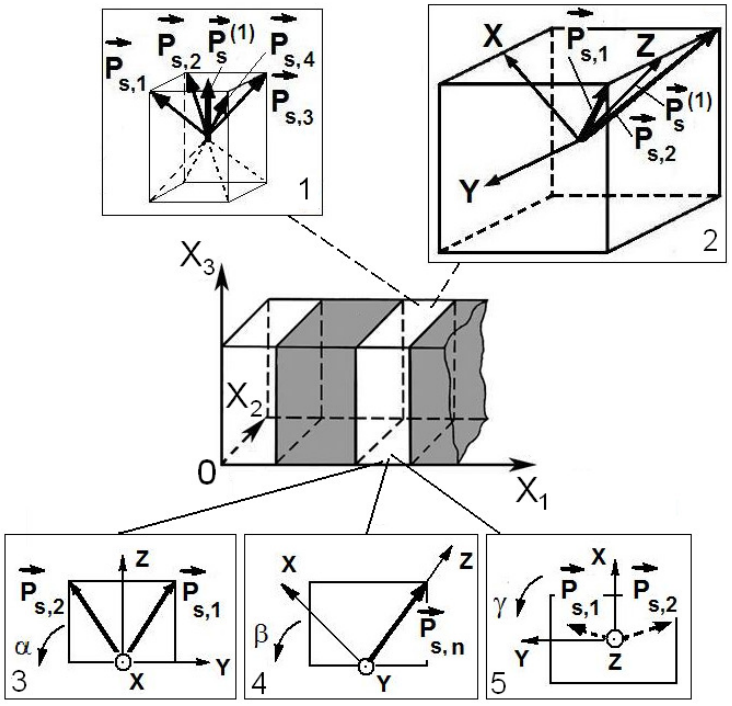

Fig. 1

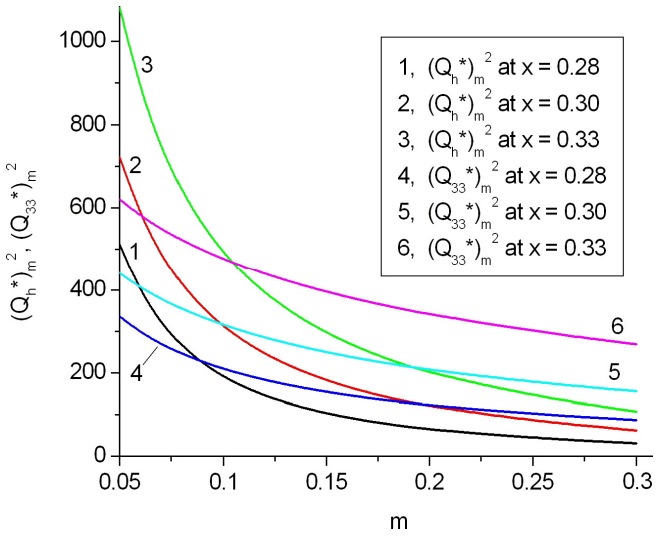

Fig. 2

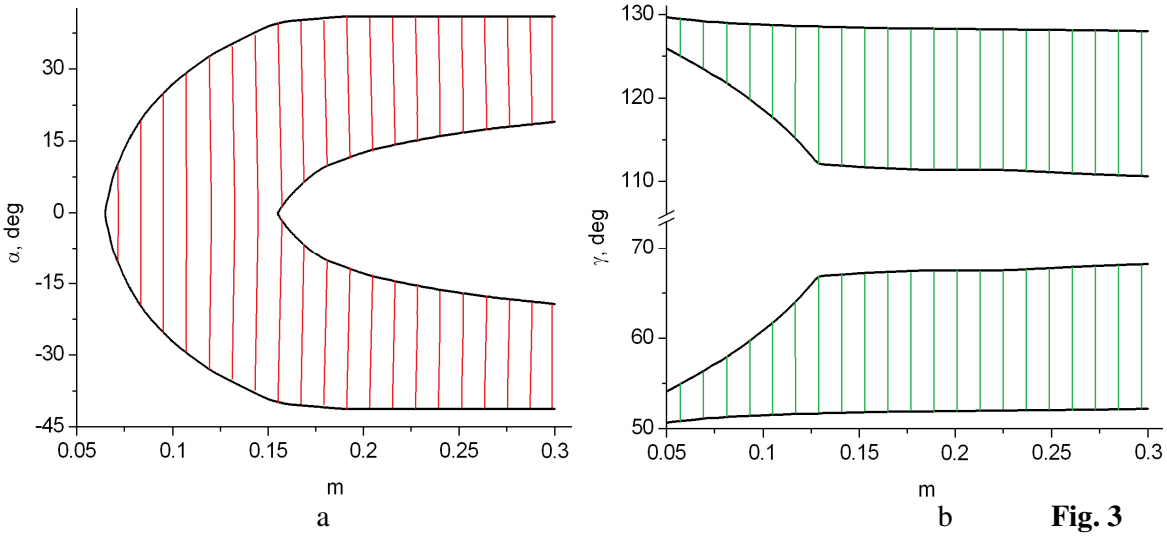

Fig. 3